Journal of Power Sources 196 (2011) 1762–1768

Contents lists available at ScienceDirect

Journal of Power Sources

journal homepage: www.elsevier.com/locate/jpowsour

Carbonate resilience of flowing electrolyte-based alkaline fuel cells

Matt S. Naughton, Fikile R. Brushett, Paul J.A. Kenis*

Department of Chemical & Biomolecular Engineering, University of Illinois at Urbana-Champaign, 600 S. Matthews Ave, Urbana, IL 61801, USA

ARTICLE INFO

Article history:
Received 1 September 2010
Received in revised form
28 September 2010
Accepted 29 September 2010
Available online 7 October 2010

Keywords:
Alkaline fuel cell
Gas diffusion electrodes
Ag cathode
Carbon dioxide
Degradation
Electrode characterization

ABSTRACT

Alkaline fuel cells (AFCs) are promising power sources due to superior kinetics and the ability to use inexpensive non-noble metal catalysts. However, carbonate formation from carbon dioxide in air has long been considered a significant hurdle for liquid electrolyte-based AFC technologies. Carbonate formation consumes hydroxyl anions, which leads to (i) reduced electrode performance if formed salts precipitate from solution and (ii) lowered electrolyte conductivity, which reduces cell performance and operating lifetime. Here, using a flowing electrolyte-based microfluidic fuel cell, we demonstrate that AFC performance can be resilient to a broad range of carbonate concentrations. Furthermore, we investigate the effects of carbonate formation rates on projected AFC operational lifetime. Results from this study will aid in the design of AFC-based power sources in light of the tradeoffs between performance, durability and cost.

1. Introduction

Rapid improvements in hydrogen storage technology are advancing fuel cells towards commercially viable portable power sources [1]. Small-scale hydrogen-fueled alkaline-based fuel cells demonstrate superior energy densities compared to rechargeable batteries offering cheaper and lighter alternatives for applications such as mobile power generators and television cameras [2]. Furthermore, metal hydrides and other metal organic frameworks provide high density hydrogen storage without the inefficiencies and safety concerns inherent to pressurized storage [3]. On-board reforming of liquid fuels, such as sodium borohydride, ammonia, or methane is another option, although the temperature and volume requirements pose a large obstacle for portable applications [3]. Alkaline fuel cells (AFCs) have cost and kinetic advantages over conventional acidic fuel cells. Many transition metals are more stable in alkaline media, allowing for cheaper catalysts (e.g. Ag and Ni) to replace the expensive Pt catalysts commonly used in acidic media [4–7]. Alkaline media also yields superior kinetics for the oxygen reduction reaction (ORR), which is the limiting reaction in acidic media [5,7,8]. Carbonate formation as well as water management have hampered mass commercialization of AFC technologies. Here we focus on the carbonate formation issue. The charge-carrying hydroxyl ions in the electrolyte react with carbon dioxide from organic fuel oxidation (i.e. methanol, formic acid) and/or air to form carbonate species via the following overall reaction:

$$2OH^- + CO_2 \rightarrow CO_3^{2-} + H_2O \quad (1)$$

This fast reaction is essentially irreversible ($K_{eq} = 7 \times 10^{25}$) and its effects are twofold. First, carbonate formation depletes hydroxyl ions from the electrolyte, which reduces electrolyte conductivity and consequently cell performance. Second, formed carbonates can precipitate within the electrode potentially blocking electrocatalytic sites. Also, these precipitants gradually decrease the hydrophobicity of the electrode backing layer leading to structural degradation and electrode flooding [9]. Carbon dioxide present in the anode or cathode feeds of an alkaline fuel cell reacts with a high conversion. For example, Gülzow et al. demonstrated that for an oxygen feed with 5 wt% CO_2, a 150 times higher concentration than found in air, more than 80% of the original CO_2 reacted after being supplied to a fuel cell without backpressure [6]. Consequently, most AFC systems employ an on-board scrubber, usually based on soda lime, to remove carbon dioxide from the oxidant stream prior to contact with the fuel cell [10]. However, these additional components increase fuel cell system volume and complexity, making this method undesirable for portable applications.

A tradeoff exists between durability and cost when designing low-temperature AFC-based power sources. The effects of carbonate formation are largely determined by the choice of electrolyte, either a liquid electrolyte or a polymeric anion-conducting membrane. Aqueous potassium hydroxide (KOH) is the most common liquid electrolyte for fuel cell applications due to the high conductivity of both potassium and hydroxide ions [11]. Such liquid electrolyte-based AFCs can operate with either stagnant or flowing

* Corresponding author. Tel.: +1 217 265 0523; fax: +1 217 333 5052.
E-mail addresses: kenis@illinois.edu, kenis@uiuc.edu (P.J.A. Kenis).

0378-7753/$ – see front matter © 2010 Elsevier B.V. All rights reserved.
doi:10.1016/j.jpowsour.2010.09.114

electrolyte streams. While stationary electrolyte configurations do not require electrolyte pumping equipment, they are more vulnerable to carbonate precipitation since the phase change is dependent on local electrolyte saturation. Operating the fuel cell at elevated temperatures (≥72 °C), at low KOH concentrations and/or with pre-scrubbed reactant streams significantly lowers the tendency for carbonate precipitation [6,9,12]. Flowing electrolyte configurations are more resistant to carbonates as precipitation is dependent on saturation of the entire electrolyte volume, but electrolyte pumping ancillaries increase system cost and complexity [13].

Recently, many research efforts focus on polymeric anion-conducting membranes to replace liquid electrolytes in AFCs. Alkaline anion exchange membranes (AAEMs) utilize a mobile anion, such as hydroxyls, and a stationary cation embedded in the polymeric membrane structure, such as quaternary ammonium [14]. Consequently, AAEMs are less susceptible to carbonate precipitation since no mobile cations are present within the membrane. However, precipitation may still occur if metal cations are present from other sources (i.e., fuel stream, component degradation by-products) [14]. Thus far, the presence of carbonates has yielded inconsistent results in AAEM-based fuel cells. For example, Piana et al. reported a significant voltage drop from the presence of CO_2 in air, whereas Adams et al. reported a small performance increase using a carbonate-doped AAEM [15,16]. The performance of AAEM-based fuel cells is also hindered by membrane-related issues, most notably water management at each electrode. Furthermore, the long term stability of AAEMs, especially at elevated temperatures, remains insufficient [17]. Whether a membrane-based approach or a flowing electrolyte based approach will be more efficient and/or cost effective is unclear at this point.

The presence of CO_2 in air has been perceived as detrimental for long term operation of alkaline liquid electrolyte fuel cells [14,16,17]. Yet, the precise effects of carbonate formation on the electrolyte at commercially relevant KOH concentrations have not been investigated quantitatively within an operating fuel cell. Previous work by Tewari et al. in a methanol/O_2 fuel cell focused solely on KOH concentrations of 1 M or less, while long-term studies by Gülzow et al. were conducted in a half-cell setup rather than in a fuel cell [6,18]. Governmental targets for the application of fuel cells in portable and stationary applications from the U.S., Japan, and the European Union all require performance degradation of less than 5–10% over the fuel cell lifetime [19,20]. An improved understanding of the extent of carbonate formation is necessary to design AFCs with the appropriate electrolyte volume for their target lifetime and/or to replace the electrolyte at appropriate intervals.

Here, we use a microfluidic hydrogen–oxygen (H_2/O_2) fuel cell with a flowing alkaline electrolyte stream [13] to study the impact of carbonates on AFC performance. External control over the flowing electrolyte in the fuel cell enables the controlled introduction of carbonate species while the individual anode and cathode losses are simultaneously monitored by an external reference electrode [21]. Initial studies without carbonate were conducted to analyze peak power density and the associated parasitic pumping losses. From the initial performances and the corresponding accelerated aging studies, the impact of carbonate formation rates on projected fuel cell lifetimes was determined and the results were compared to reported values in the literature.

2. Experimental

2.1. Gas diffusion electrode preparation

Commercially available Pt/C (50% mass on Vulcan carbon, E-Tek) or Ag/C (60% mass on Vulcan carbon, E-Tek) were used as electrode catalysts. A 40 wt% loading of polytetrafluoroethylene (PTFE, Aldrich) was used as the catalyst binder such that catalyst inks were prepared by mixing 2 mg of Pt/C or 6.7 mg of Ag/C and 1.3 mg or 4.5 mg PTFE powder, respectively [13]. 100 μl of DI water and 150 μl of isopropyl alcohol were added as carrier solvents. The catalyst inks were sonicated (Branson 3510) for 1 h to obtain a uniform mixture, which was then painted onto the hydrophobized carbon side of a Toray carbon paper gas diffusion layer (EFCG "S" type electrode, E-Tek) to create a gas diffusion electrode (GDE). The GDE was sintered under a nitrogen atmosphere at 330 °C for 20 min in a pre-heated tube furnace (Lindberg/Blue) followed by hot pressing at a pressure of 340 psi and a temperature of 120 °C. For the microfluidic H_2/air fuel cell, the final catalyst loading was 4 mg cm^{-2} of Ag (60% mass Ag) for the cathode and 1 mg cm^{-2} of Pt (50% mass Pt) for the anode. For the microfluidic H_2/O_2 fuel cell, the final catalyst loading was 1 mg cm^{-2} of Pt (50% mass Pt) for both electrodes.

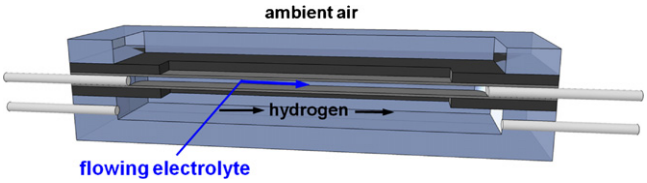

Fig. 1. Diagram of a microfluidic fuel cell with a flowing electrolyte. In the H_2/air setup shown here, air passively diffuses to the cathode while pure hydrogen is fed to the anode at 10 sccm.

2.2. Fuel cell assembly and testing

To assemble the fuel cell, shown in Fig. 1, the cathode (Pt/C or Ag/C) and the anode (Pt/C) were placed on the opposite sides of a 0.15 cm thick polymethylmethacrylate (PMMA) window, such that the catalyst-coated GDE sides face the 3-cm long and 0.33-cm wide window machined in PMMA [22]. The microfluidic chamber volume was 0.15 ml. The window has one inlet and one outlet from the side for the electrolyte flow, aqueous solutions of either potassium hydroxide (KOH, Mallinckrodt, 88%, balance of H_2O) or potassium carbonate (K_2CO_3, Fisher Chemical, 99.8%). Two 1-mm thick graphite windows were used as current collectors. For the air-breathing configuration, on the anode side a polycarbonate gas flow chamber (5 cm (L) × 1 cm (W) × 0.5 cm (H)) was used to introduce hydrogen gas (laboratory grade, S.J. Smith), at 10 sccm, and on the cathode side, a polycarbonate window was positioned over the graphite current collector to enable oxygen to diffuse from the ambient environment. The low hydrogen flow rate minimizes the pressure differential across the microfluidic channel but also maintains uniform reactant conditions along the GDE length [22]. For the H_2/O_2 configuration, polycarbonate gas flow chambers were used to introduce both hydrogen and oxygen gases (laboratory grade, S.J. Smith), at 50 sccm each. In both cases, the multilayer assemblies were held together with binder clips (Highmark). Fuel cell testing was conducted using a potentiostat (Autolab PGSTA-30, EcoChemie) at room temperature. For all studies, electrolyte flow rate was maintained at 0.3 ml min^{-1} using a syringe pump (2000 PHD, Harvard Apparatus) [13]. Prior to experiments using the Ag cathode, the fuel cell was operated at 0.3 V for 20 min to activate the catalyst [6]. Fuel cell polarization curves were obtained by measuring steady-state currents at different cell potentials using General Purpose Electrochemical System (GPES) software (EcoChemie). The exposed geometric surface area of the electrode (1 cm^2) was used to calculate the current and power densities. A reference electrode (Ag/AgCl in saturated NaCl, BASi) was placed at the outlet of the electrolyte stream to allow for the independent analysis of polarization losses on the cathode and the anode [21]. After each experiment, the fuel cell was disassembled and the electrodes were rinsed with deionized water, then dried under a laboratory fume hood.

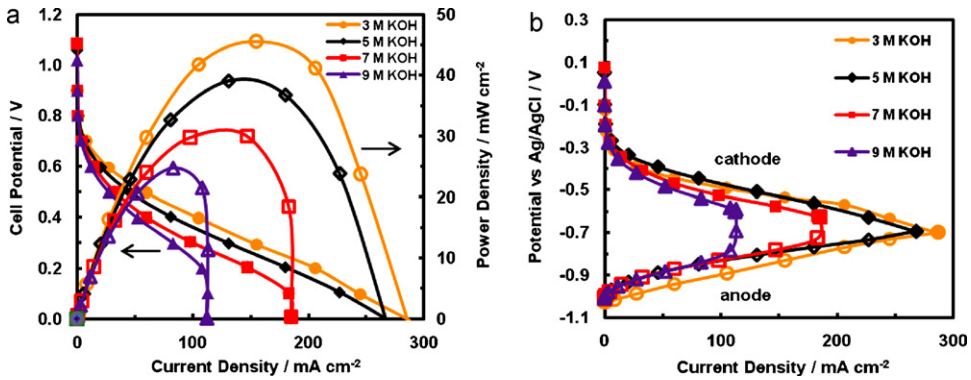

Fig. 2. (a) Power density curves and (b) corresponding polarization curves for an air-breathing fuel cell operated at varying KOH concentrations. Electrodes: Pt/C (1 mg Pt cm^{-2}) anode and Ag/C cathode (4 mg Ag cm^{-2}). Electrolyte flow rate: 0.3 ml min^{-1}. H_2 feed: 10 sccm. O_2 feed: air-breathing. At room temperature.

2.3. Conductivity measurement

The room temperature conductivity of electrolyte solutions was measured with an Orion 4 star pH/conductivity meter (Thermo Scientific) using a two-electrode conductivity cell (Duraprobe 018020MD). Before measurement, the conductivity cell was triple rinsed with deionized water and calibrated with a 1 M KCl solution with conductivity 111.9 mS cm^{-1}. Conductivity measurements were taken in triplicate and the average of the three values was used for the IR-corrections.

3. Results and discussion

3.1. Effect of KOH concentration on cell performance

The performance of the microfluidic H_2/air fuel cell, operated with a Pt/C anode and Ag/C cathode, was first investigated as a function of electrolyte concentrations (3, 5, 7, and 9 M KOH). Selecting the optimum KOH concentration in an alkaline fuel cell involves consideration of tradeoffs between kinetics, conductivity, and viscosity, which all change as a function of concentration. Previous studies using a microfluidic H_2/O_2 fuel cell by Brushett et al. showed inferior performance at 1 M KOH; specifically, only 56% of the peak power density achieved with 3 M KOH, due to both reduced electrolyte conductivity and lower Ag/C cathode oxygen reduction activity at that concentration [13]. Fig. 2a shows polarization and power density curves for the microfluidic fuel cell performance operating with KOH concentrations of 3–9 M. The fuel cell generated peak power densities of 47, 39, 29, and 25 mW cm^{-2} for 3, 5, 7, and 9 M KOH, respectively. Thus, optimal performance is observed at 3 M KOH. Performance decreases with increasing electrolyte concentration despite increasing electrolyte conductivity. The individual electrode polarization curves (Fig. 2b) reveal reduced anode performance as the main cause for lowered overall fuel cell performance at higher KOH concentrations. The anode performance losses at higher KOH concentrations are mainly due to increased electrolyte viscosity hampering water management, which leads to anode flooding at high current densities [23,24]. Another anodic performance-limiting factor is competitive hydroxyl ion absorption at higher electrolyte concentrations, which blocks the adsorption of hydrogen species and reduces electrode performance [25,26]. Additional hydroxyl ions only improve electrode kinetics up to a certain threshold KOH concentration. Finally, at higher electrolyte concentrations, another possible limiting factor is high counterion (K^+) concentrations, which can cause anode shielding. These effects outweigh the decreased hydrogen oxidation equilibrium potential from the increased pH (Nernstian shift). These observations are in good agreement with results obtained in a microfluidic H_2/O_2 fuel cell operated with Pt/C electrodes [23].

The decreasing cathode performance with increasing KOH concentration may be attributed to the downward Nernstian potential shift at higher pH (particularly visible for 9 M KOH), increased hydroxyl adsorption at the catalytic sites, and the aforementioned increase in electrolyte viscosity at higher KOH concentration [5]. In summary, for this microfluidic configuration, optimal performance at RT was observed at 3 M KOH where the effects of high electrolyte conductivity and lower electrolyte viscosity balance. Note that at elevated temperatures, this balance may shift to higher KOH concentrations since increased temperatures reduce electrolyte viscosity and improve electrode kinetics.

To determine overall power output and design feasibility of AFCs with flowing electrolyte, parasitic losses associated with electrolyte pumping must be quantified. Pumping losses are a function of both the pumping setup and the electrolyte composition. The well-known laminar flow solution for fully developed pipe flow and the Bernoulli equation [27] were used to calculate the parasitic losses for the microfluidic cell used here (Table 1). For these calculations, the pumping efficiency was assumed to be 40%.

As KOH concentration increases, electrolyte viscosity also increases but peak power density decreases. Consequently, at higher KOH concentrations, pumping requirements consume a greater percentage of the fuel cell power output. The 3 M KOH solution has the lowest power loss, while the 9 M KOH solution has the highest power loss. This behavior can be attributed to the higher viscosity for the 9 M KOH solution and the lower peak power density. The results suggest that a microfluidic setup is viable as a portable fuel cell, with 3 M being the optimal KOH concentration for our operating conditions in the absence of contaminants such as carbonates formed from CO_2.

3.2. Effect of carbonate formation on Pt and Ag cathode performance

We previously demonstrated the ability of a flowing electrolyte stream between the electrodes to remove formed carbonates from Pt/C electrode surfaces [23]. In those studies, neat CO_2 was introduced on the anode side of a microfluidic fuel cell with a stationary electrolyte. After prolonged carbonate poisoning, we demonstrated

Table 1
Parasitic power losses with no carbonate formation.

KOH (M)	Maximum power density (mW cm^{-2})	Power loss (mW cm^{-2})	% power loss
3	47	4.4	9.4
5	39	5.8	14.7
7	29	7.7	26.2
9	25	10.2	41.0

Table 2
Tested KOH concentrations.

KOH (M)	K_2CO_3 (M)
3.0	0.00
2.5	0.25
2.0	0.50
1.5	0.75
1.0	1.0
0.50	1.3
0.00	1.5

that the flowing electrolyte was able to remove any precipitated carbonates from the anode surface, fully restoring fuel cell performance. While these experiments were performed in a microfluidic H_2/O_2 fuel cell with Pt/C electrodes, the results are applicable to other microfluidic configurations, such as the air-breathing cell used here, as the effect is electrolyte-dependent.

Based on the demonstrated ability of a flowing electrolyte stream to dissolve carbonates, thereby fully restoring fuel cell performance, we can study the problem of carbonate formation systematically by varying the composition of the electrolyte stream from 3 M KOH to 1.5 M K_2CO_3 in steps of 0.5 M KOH (Table 2). Recall that one carbonate forms by the reaction of two hydroxyls with one CO_2 (Eq. (1)). The effects of electrolyte composition on fuel cell peak power densities were investigated in two microfluidic configurations, a high performance H_2/O_2 fuel cell with Pt/C electrodes and a H_2/air fuel cell with Pt/C anode and Ag/C cathode (Fig. 3). Here, we define a parameter, the 90% threshold, as the KOH concentration above which the peak power density is at least 90% of the initial value, adhering to governmental targets [19].

Fig. 3 shows a steeper drop-off in performance for the H_2/O_2 configuration compared to the air-breathing configuration, which is likely due to the higher demand on the anode in the H_2/O_2 experiment making the hydroxyl loss more significant, since the conductivity losses and the viscosity increases are the same for both setups. Both configurations show a fairly small initial decline in performance due to decreased electrolyte conductivity, and then show an increasingly steep drop in performance as the hydroxyl losses begin to negatively impact anode kinetics. This sharp drop occurs between 1.5 and 2 M KOH (0.5–0.75 M K_2CO_3) for the H_2/O_2 setup and between 1 and 1.5 M KOH (0.75–1 M K_2CO_3) for the air-breathing setup. The final peak power densities, observed at 1.5 M

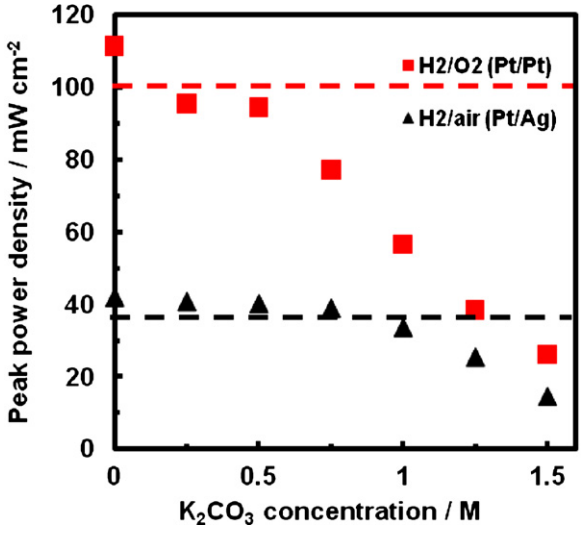

Fig. 3. Fuel cell peak power density as a function of K_2CO_3 formed for the microfluidic fuel cell operated with a forced O_2 stream or with quiescent air. The horizontal dashed lines indicate the 90% level of the initial power density for each run. Electrolyte flow rate: 0.3 ml min^{-1}. H_2 and O_2 feed: 50 sccm. At room temperature.

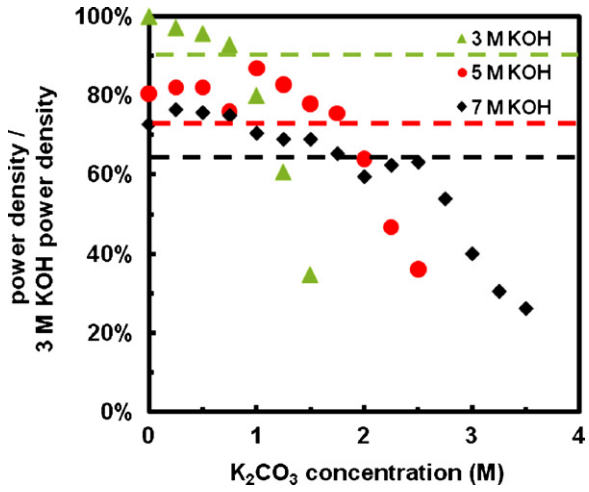

Fig. 4. Normalized power density of a H_2/air fuel cell operated at different KOH concentrations as a function of [K_2CO_3] formed. The horizontal dashed lines indicate the 90% level of the initial power density for each run. Electrodes: Pt/C (1 mg Pt cm^{-2}) anode and Ag/C cathode (4 mg Ag cm^{-2}). Electrolyte flow rate: 0.3 ml min^{-1}. H_2 feed: 10 sccm. O_2 feed: air-breathing. At room temperature.

K_2CO_3, are 23% and 34% of the peak power densities, observed in 3 M KOH, for the H_2/O_2 and the air-breathing setups, respectively. These results indicate that the H_2/O_2 configuration is more sensitive to the presence of carbonates than the air-breathing configuration, which retains more than 90% peak power density until more than 50% of the KOH is reacted to form carbonates. Consequently, we used the microfluidic H_2/air cell fuel operating with a Pt/C anode and a Ag/C cathode for the rest of our experiments.

3.3. Effect of carbonate formation at different KOH concentrations

Since the electrolyte composition changes over the fuel cell lifetime, a 3 M KOH starting concentration may not be optimal for extended operation. To investigate the sensitivity of various alkaline electrolyte concentrations to carbonate formation, we studied microfluidic H_2/air fuel cell performance utilizing initial electrolyte concentrations of 3, 5, and 7 M KOH (Fig. 3) over the course of six days. For each concentration, carbonates were introduced in 0.25 M increments. Results were normalized daily to a 3 M KOH trial conducted that day to eliminate any error from electrode decay (due to loss of hydrophobicity) over the course of experiments. To compare the results of varying KOH concentrations, we define a second parameter, $C_{optimum}$, as the range of K_2CO_3 formation where a certain KOH concentration gives the highest comparative fuel cell performance.

Fuel cells operated at higher initial KOH concentrations demonstrate greater carbonate tolerances (Fig. 4), since their maximum power densities decrease at a slower rate than fuel cells operated with 3 M KOH. This slower performance drop is due to the higher initial hydroxide ion concentrations which increase resilience to carbonate formation by maintaining high electrolyte conductivities (Table 3). Note that at first this long-term advantage of carbonate resilience when operating at 5 or 7 M KOH is offset by the

Table 3
Performance degradation as a function of carbonate formation.

Configuration	KOH (M)	90% threshold (M K_2CO_3)	$C_{optimum}$ (M K_2CO_3)
H_2/O_2	3	0	N/A
H_2/air	3	0.75	0–1
H_2/air	5	1.75	1–2
H_2/air	7	1.75	2–3.5

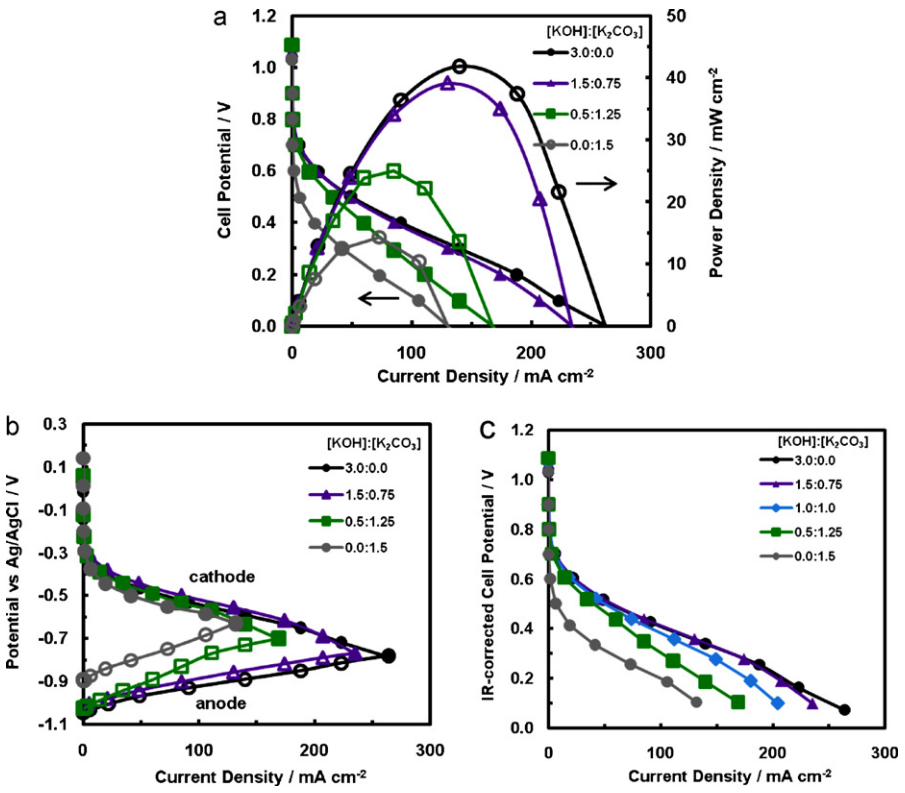

Fig. 5. (a) Polarization and power density curves, as well as corresponding (b) anode and cathode polarization curves, and (c) IR-corrected polarization curves for a H_2/air cell with a Pt anode and a Ag cathode for different KOH over K_2CO_3 ratios. Electrodes: Pt/C (1 mg Pt cm^{-2}) anode and Ag/C cathode (4 mg Ag cm^{-2}). Electrolyte flow rate: 0.3 ml min^{-1}. H_2 feed: 10 sccm. O_2 feed: air-breathing. At room temperature.

lower fuel cell peak power densities compared to the initial peak power density observed when operating at 3 M KOH (e.g. Fig. 1). A sharp drop-off in power density is observed at about 1.5 M KOH for each initial electrolyte concentration due to reduced anode kinetics and electrolyte conductivity at this low KOH concentration. The individual electrode polarization curves (Fig. 5b) demonstrate the diminished anode kinetics at KOH concentrations lower than 1.5 M, while the overlay of the 3 M KOH and 1.5 M KOH IR-corrected polarization curves demonstrates that the performance decrease at higher KOH concentrations is only due to conductivity losses (Fig. 5c). In addition to reduced kinetics, carbonate blocking of active sites and reduced local pH at the anode surface may also contribute to the reduced performance.

Table 3 demonstrates that 7 M KOH is undesirable for operation above the 90% performance threshold, since the lower initial performance means that $C_{optimum}$ is not reached until the conductivity loss reduces the power density below the 90% level. Cells operated with 3 and 5 M KOH are both promising for different niches. For example, fuel cells operated with 3 M KOH work well with carbonate formation up to 0.75 M K_2CO_3, if the inlet gas streams are scrubbed and/or if the electrolyte is replaced frequently. By contrast, operation with 5 M KOH is superior for longer-term applications up to 1.75 M K_2CO_3, presumably making it more suitable for configurations that do not scrub the feed streams.

3.4. Comparison with literature

In an earlier study, Gülzow et al. investigated the carbonate sensitivity of a Ag/PTFE electrode in a half-cell setup operating at 80 °C using a stagnant 7.1 M KOH electrolyte [6]. Experiments were conducted over 3000 h using an inlet gas stream consisting of either 95 wt% O_2 and 5 wt% CO_2, which is 150× the concentration of CO_2 in ambient air, or 100% O_2 to investigate the extent and effects of carbonate formation on performance. Near identical half-cell performances were observed in both experiments, and the authors concluded that "CO_2 in air is not really a problem for AFCs". As this work appeared to disagree with our findings, we performed a comparative study of our respective experiments. Via titration analysis, Gülzow et al. determined that 0.3 M K_2CO_3 had formed over the course of 600 h, which stoichiometrically corresponds to 6.5 M KOH [6]. Gülzow et al. also reported that the carbonate formation rate can be assumed to be roughly constant over the experiment since the CO_2 concentration in the O_2 stream remains constant [6]. Thus, over the course of 3000 h, the same rate of carbonate formation would yield an electrolyte composition of 1.3 M K_2CO_3 and 4.3 M KOH. The effects of a similar amount of carbonate formation can be simulated in our microfluidic system using 7.0 M KOH. Fig. 6 demonstrates that the effects of altering the electrolyte composition from 7.0 M KOH to 4.3 M KOH and 1.3 M K_2CO_3 are limited to a less than 5% decrease in maximum power density. Interestingly, despite very different experimental setups including temperature, oxygen delivery method, and catalysts employed, our result is in close agreement with the observations of Gülzow, which indicates the broad applicability of our experimental findings.

3.5. Electrolyte volume vs. cell lifetime

Ideally, one would like the electrolyte volume in an AFC to be large in order to minimize the change in concentration for a given rate of carbonate and water formation. However, given the size and weight constraints for portable systems, such ideal volumes may not be feasible. For example, the experiments previously described by Gülzow et al. were conducted using 1.5 l of electrolyte [6]. Unfortunately, this volume is far greater than the volume that could be used in a "portable" fuel cell system, as even laptop batteries are approximately 300 ml in total volume [28]. However, the Gülzow

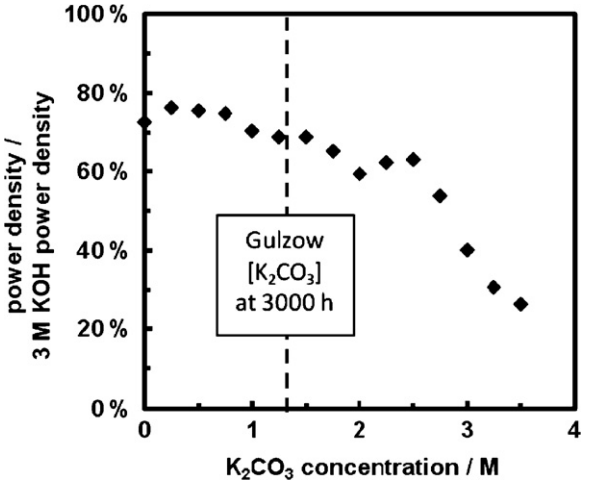

Fig. 6. Normalized power density of a H_2/air cell with a Pt anode and a Ag cathode as a function of [K_2CO_3] formed for an initial electrolyte concentration of 7 M KOH. Electrodes: Pt/C (1 mg Pt cm^{-2}) anode and Ag/C cathode (4 mg Ag cm^{-2}). Electrolyte flow rate: 0.3 ml min^{-1}. H_2 feed: 10 sccm. O_2 feed: air-breathing. At room temperature.

Table 4
Projected lifetimes based upon carbonate formation.

KOH (M)	90% threshold (h)	$t_{optimal}$ (h)
3	1700	0–2200
5	3900	2200–4500
7	3900	4500–7800

experiments were run using 150× the normal concentration of CO_2, which can be assumed to translate into 150× the normal rate of carbonate formation based on the high conversion of any CO_2 fed into the alkaline half-cell [6]. Scaling the 1.5 l electrolyte volume down by a factor of 150 yields a 10 ml electrolyte volume. Thus, operating our microfluidic cell with 10 ml of electrolyte should exhibit changes in composition comparable to operating with an oxygen stream with 5 wt% CO_2 for 1.5 l of electrolyte. Furthermore, Ko et al. demonstrated that the initial rate of change in carbonate concentration is roughly linear for KOH solutions exposed to CO_2 from ambient air [29]. By applying this result to our experimental observation, operating lifetimes can be projected for a microfluidic fuel cell operated with 10 ml electrolyte. However, this 10 ml volume is much larger than the 0.15 ml volume of the microfluidic fuel cell chamber, which necessitates a flowing electrolyte for long term operation. Here, we define $t_{optimal}$ to be the time range during which different KOH concentrations give the highest performance (Table 4).

As shown in Table 4, microfluidic H_2/air fuel cells with 3 M KOH are projected to operate for 1700 h while maintaining 90+% of the maximum performance. We predict that using a higher electrolyte concentration (≥5 M KOH) would allow for lifetimes of up to 3900 h, due to its higher capacity to absorb CO_2. In comparison, the 0.15 ml chamber volume alone would yield a 90% threshold of only 26 h for 3 M KOH, which is most likely too short for most applications.

4. Conclusions

Here, we reported on a series of experiments to determine the effects of varying electrolyte compositions on the peak performance of an alkaline microfluidic fuel cell. While a H_2/O_2 setup outperformed an air-breathing setup due to superior kinetics and reactant mass transfer, this high-performance configuration was found to be less resilient to carbonate formation. We found that while microfluidic H_2/air fuel cells operated with 3 M KOH demonstrated the highest power densities, they were also the least tolerant of carbonate formation, projected to be resilient for 1900 h of operation in ambient air. Furthermore, increasing the KOH concentration above 3 M increases resilience to carbonate formation with the projected performance dropping by less than 10% for 3900 h of operation in ambient air. While long-term durability testing would still be needed to verify these results, the initial predictions for AFCs as portable power sources are promising.

Understanding these carbonate formation effects provides guidelines for the design and operation of microscale flowing electrolyte AFCs for portable applications. In particular, the electrolyte volume is a key design component to mitigate carbonate formation; the operational lifetime will increase proportionally with the electrolyte volume. With sufficient electrolyte volume, the AFC lifetime then hinges on the degradation of the other components most notably the electrodes which decay rapidly, resulting in a ∼15% performance drop over the course of our experiments at elevated KOH concentrations. Developing a deeper understanding of and quantifying these electrode degradation patterns is necessary in order to improve flowing electrolyte AFC lifetimes.

Acknowledgments

We gratefully acknowledge funding from the Department of Energy (DE-FG02005ER46260) and from the National Science Foundation (CAREER grant CTS 05-47617). We also acknowledge H.-R. "Molly" Jhong for assistance with experimentation.

References

[1] C.K. Dyer, J. Power Sources 106 (2002) 31–34.
[2] C. Potera, Environ. Health Perspect. 115 (2007) A38–A41.
[3] A. Kundu, J.H. Jang, J.H. Gil, C.R. Jung, H.R. Lee, S.H. Kim, B. Ku, Y.S. Oh, J. Power Sources 170 (2007) 67–78.
[4] C. Coutanceau, L. Demarconnay, C. Lamy, J.M. Leger, J. Power Sources 156 (2006) 14–19.
[5] J.S. Spendelow, A. Wieckowski, Phys. Chem. Chem. Phys. 9 (2007) 2654–2675.
[6] E. Gülzow, M. Schulze, J. Power Sources 127 (2004) 243–251.
[7] F.R. Brushett, M.S. Thorum, N.S. Lioutas, M.S. Naughton, C. Tornow, H.-R.M. Jhong, A.A. Gewirth, P.J.A. Kenis, J. Am. Chem. Soc. (2010) (Web published).
[8] G.F. McLean, T. Niet, S. Prince-Richard, N. Djilali, Int. J. Hydrogen Energy 27 (2002) 507–526.
[9] A. Rolla, A. Sadkowski, J. Wild, P. Zoltowski, J. Power Sources 5 (1980) 189–196.
[10] M. Cifrain, K.V. Kordesch, J. Power Sources 127 (2004) 234–242.
[11] CRC Handbook of Chemistry and Physics, CRC Press/Taylor, Boca Raton, FL, 2009.
[12] M. Al-Saleh, S. Gültekin, A. Al-Zakri, H. Celiker, J. Appl. Electrochem. 24 (1994) 575–580.
[13] F.R. Brushett, W.P. Zhou, R.S. Jayashree, P.J.A. Kenis, J. Electrochem. Soc. 156 (2009) B565–B571.
[14] S.F. Lu, J. Pan, A.B. Huang, L. Zhuang, J.T. Lu, Proc. Natl. Acad. Sci. U.S.A. 105 (2008) 20611–20614.
[15] M. Piana, M. Boccia, A. Filpi, E. Flammia, H.A. Miller, M. Orsini, F. Salusti, S. Santiccioli, F. Ciardelli, A. Pucci, J. Power Sources 195 (2010) 5875–5881.
[16] L. Adams, S. Poynton, C. Tamain, R. Slade, J. Varcoe, ChemSusChem 1 (2008) 79–81.
[17] J.R. Varcoe, R.C.T. Slade, Fuel Cells 5 (2005) 187–200.
[18] A. Tewari, V. Sambhy, M. Urquidi MacDonald, A. Sen, J. Power Sources 153 (2006) 1–10.
[19] Multi-Year Research, Development and Demonstration Plan: Planned Program Activities for 2005–2015, 2007. Retrieved from http://www1.eere.energy.gov/hydrogenandfuelcells/mypp/ (accessed October 9, 2009).
[20] R. Borup, J. Meyers, B. Pivovar, Y.S. Kim, R. Mukundan, N. Garland, D. Myers, M. Wilson, F. Garzon, D. Wood, P. Zelenay, K. More, K. Stroh, T. Zawodzinski, J. Boncella, J.E. McGrath, M. Inaba, K. Miyatake, M. Hori, K. Ota, Z. Ogumi, S. Miyata, A. Nishikata, Z. Siroma, Y. Uchimoto, K. Yasuda, K.-i. Kimijima, N. Iwashita, Chem. Rev. 107 (2007) 3904–3951.
[21] E.R. Choban, P. Waszczuk, P.J.A. Kenis, Electrochem. Solid-State Lett. 8 (2005) A348–A352.

[22] R.S. Jayashree, M. Mitchell, D. Natarajan, L.J. Markoski, P.J.A. Kenis, Langmuir 23 (2007) 6871–6874.
[23] F.R. Brushett, M.N. Naughton, P.J.A. Kenis, unpublished results.
[24] Viscosity (cps) of Aqueous KOH (wt%) Solutions, 2010. Retrieved from http://koh.olinchloralkali.com/TechnicalInformation/KOH%20Viscosity.pdf (accessed August 16, 2010).
[25] N.M. Markovic, B.N. Grgur, P.N. Ross, J. Phys. Chem. B 101 (1997) 5405–5413.
[26] F. Alcaide, E. Brillas, P.-L. Cabot, J. Electrochem. Soc. 152 (2005) E319–E327.
[27] F.M. White, Fluid Mechanics, 5th ed., McGraw-Hill, New York, 2003.
[28] Battery features, 2008. Retrieved from http://www.todaybattery.com/ (accessed October 9, 2009).
[29] H.-W. Ko, H.-K. Juang, J. Appl. Electrochem. 13 (1983) 725–730.